

## High Signal Intensity of the Cochlear Modiolus on Unenhanced T1-Weighted Images in Classical Infratentorial Superficial Siderosis

Eiji Matsusue,\* Chie Inoue,\* Kensuke Matsumoto,\* Tomohiko Tanino,\* Kazuhiko Nakamura\* and Shinya Fujii†

\*Department of Radiology, Tottori Prefectural Central Hospital, Tottori 680-0901, Japan, and †Division of Radiology, Department of Multidisciplinary Internal Medicine, School of Medicine, Tottori University, Yonago 683-8503, Japan

### ABSTRACT

**Background** Superficial siderosis (SS) results from chronic bleeding in the subarachnoid space. SS can be classified as infratentorial SS (i-SS) and supratentorial SS (s-SS). The cochlear modiolus (CM) normally shows low signal intensity (SI) on T1-weighted images (T1WI). We noticed persistently high SI of the CM on unenhanced thin-sliced T1WI in patients with i-SS. The purpose of this study was to evaluate the correlation between SS and high SI of the CM on unenhanced T1WI.

**Methods** This retrospective study analyzed three cases with i-SS, eight cases with s-SS, and 23 normal controls (NC) evaluated on unenhanced thin-sliced T1WI with a three-dimensional spoiled gradient-recalled echo sequence. CM-T1SI scores of 0, 1, and 2 indicated low, iso, and high SI, respectively. In cases with scores of 2 evaluated several times, all scores were reviewed for each case. The CM-T1SI ratio was defined as the contrast ratio between the CM and the cerebellum. Differences between the three groups were statistically analyzed based on the CM-T1SI score and ratio. Receiver operative curve (ROC) analysis was used to determine the cut-off values for differentiating the i-SS group from the NC group based on the CM-T1SI ratio.

**Results** Two patients with i-SS had a score of 2 on all evaluations. The CM-T1SI score and ratio differed significantly between the i-SS and NC groups. The accuracy of the CM-T1SI ratio for discriminating i-SS from NC was 98.9% at a cutoff value of 0.628.

**Conclusion** High SI of the CM on unenhanced T1WI can be an additional characteristic finding of i-SS.

**Key words** cochlear modiolus; magnetic resonance imaging; superficial siderosis; T1-shortening; SPGR

Superficial siderosis (SS) is a rare disorder that results from chronic or intermittent bleeding into the subarachnoid space, leading to the deposition of hemosiderin in the subpial layers of the brain and spinal cord.<sup>1–3</sup> SS is observed on T2-weighted images (T2WI) in magnetic resonance imaging (MRI) as a typical low-intensity outlining of the brain surface. T2\*-weighted images (T2\*WI) and susceptibility-weighted images (SWI) have a higher sensitivity for hemosiderin deposition.<sup>3, 4</sup>

SS can be divided into two types: classical infratentorial SS (i-SS) and cortical supratentorial SS (s-SS).<sup>5</sup> i-SS mainly affects the brainstem and cerebellum, with diffuse and symmetrical margins. The causes of hemorrhage in i-SS include tumors, vascular abnormalities, injury, and dural defects.<sup>4, 6, 7</sup> s-SS shows a characteristic curvilinear pattern that preferentially affects cerebral convexities.<sup>4</sup> s-SS can have traumatic or non-traumatic origins, including cerebral amyloid angiopathy.<sup>8</sup> Patients with i-SS may present with slowly progressive and irreversible cerebellar ataxia, sensorineural hearing loss, myelopathy, and/or dementia.<sup>7, 9</sup> Patients with s-SS may present with transient focal neurological episodes, focal seizures, and/or migrainous auras.<sup>8, 10, 11</sup> Many cases of SS are asymptomatic and become symptomatic only with extensive widespread iron deposition.<sup>9</sup>

The cochlea, vestibule, and semicircular canals comprise the labyrinth. The cochlear modiolus (CM) is a conical-shaped structure consisting of spongy bone located in the center of the cochlea. The otic labyrinth lumen normally has a relatively low signal intensity (SI) on T1WI, intermediate between the cerebrospinal fluid (CSF) and the brain.<sup>12</sup> In our institution, we coincidentally noticed persistently high SI of the CM for years on unenhanced thin-sliced T1WI, using a three-dimensional spoiled gradient-recalled echo sequence (3D-SPGR) in patients with i-SS, although this finding was not discussed in previous reports. We hypothesized that hyperintensity of the CM on unenhanced T1WI was associated with SS.

Thus, this study evaluated the correlation between SS and high SI of the CM on unenhanced thin-sliced T1WI.

Corresponding author: Eiji Matsusue, MD, PhD  
matsusuee@tp-ch.jp

Received 2022 August 2

Accepted 2022 September 2

Online published 2022 October 19

Abbreviations: Az, area under the ROC curve; CM, cochlear modiolus; CR, contrast ratio; CSF, cerebrospinal fluid; FOV, field of view; i-SS, infratentorial SS; MRI, magnetic resonance imaging; NC, normal control; ROC, receiver operative curve; ROI, region of interest; SI, signal intensity; SS, superficial siderosis; s-SS, supratentorial SS; SWI, susceptibility-weighted images; TE, echo time; TR, repetition time; T1WI, T1-weighted images; T2\*WI, T2\*-weighted images; 3D-SPGR, three-dimensional spoiled gradient-recalled echo sequence

**Table 1. Demographics of patients in the i-SS, s-SS, and NC groups**

	i-SS group	s-SS group	NC group
Number	3	8	23
Age (years), mean $\pm$ SD	63 $\pm$ 15	75 $\pm$ 8	71 $\pm$ 12
Female/Male	2/1	1/7	7/16

i, infratentorial; NC, normal control; s, supratentorial; SD, standard deviation; SS, superficial siderosis.

## MATERIALS AND METHODS

### Patients

This retrospective study identified 96 patients with SS showing low SI of the subarachnoid spaces on T2WI and T2\*WI using 3-Tesla systems between April 2014 and April 2022. This study analyzed 11 patients who underwent 3D-SPGR T1WI; the remaining 85 patients (66 patients with s-SS and 19 patients with i-SS) were excluded due to the evaluation of fast spin-echo T1WI using 5-mm-thick sections. i-SS was defined as the appearance of bilateral well-defined curvilinear homogeneous low SI on T2WI and T2\*WI over the superficial surface of at least two of the following regions: (1) brainstem, (2) cerebellum, and (3) spinal cord or craniocervical junction.<sup>7</sup> In addition, s-SS was defined as the appearance of curvilinear low SI on T2WI and T2\*WI over the superficial surface of the cerebral cortices, distinct from the vessels. Using these criteria, three and eight of the 11 patients were diagnosed with i-SS and s-SS, respectively. In addition, another 23 normal subjects without any other primary diseases or abnormalities on T2\*WI and 3D-SPGR T1WI served as the normal controls (NCs). The demographic and imaging characteristics of the i-SS, s-SS, and NC groups are shown in Tables 1 and 2.

The institutional review board of our hospital approved this study (approval number 2022-20), which waived the requirement for written informed consent from the participants due to the retrospective nature of the study.

### Image acquisition and analysis

MRI was performed in all 34 cases using a 3-Tesla MRI system (Philips Ingenia, Best, The Netherlands) with an eight-channel phased-array head coil.

Axial images were acquired parallel to the anterior commissure-posterior commissure line, following the protocol for adult brain imaging at our hospital: T1-weighted 3D-SPGR echo sequence, repetition time/echo time (TR/TE), 7.0/2.4 ms; slice thickness, 0.7 mm; field of view (FOV), 240  $\times$  240 mm; matrix, 360  $\times$  354; T2\*-weighted multi-echo gradient-recalled echo sequence,

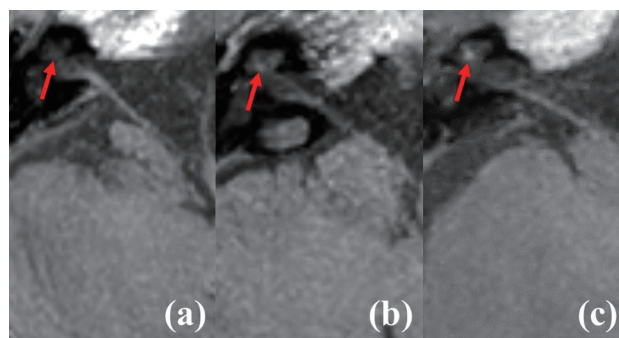


**Fig. 1.** Examples of scoring cochlear modiolus (CM) signal intensity (SI) on T1-weighted images (T1WI). (a) The SI of the CM (arrow) is scored as 0 when the SI is lower than that of the cranial nerves or the cerebellum. (b) The SI of the CM (arrow) is scored as 1 when the SI is equal to that of the cranial nerves or the cerebellum. (c) The SI of the CM (arrow) was scored as 2 when the SI was brighter than that of the cranial nerves or the cerebellum.

TR/TE, 510/20 ms; section thickness, 5 mm; FOV, 200  $\times$  187 mm; matrix, 256  $\times$  217; T2-weighted fast spin-echo sequence, TR/TE, 4000/85 ms; section thickness, 5 mm; FOV, 240  $\times$  220 mm; matrix, 380  $\times$  270.

The MRI data were interpreted using a clinical viewer (F-report; FUJIFILM, Tokyo, Japan). The images were analyzed by one radiologist (E.M., with 25 years of experience in head and neck MRI). For the qualitative evaluation of CM-T1SI scores, each SI of the bilateral CM on 3D-SPGR T1WI was scored as 0 when the SI of the CM was lower than that of the cranial nerves or cerebellum, 1 when the SI was equal to that of the cranial nerves or cerebellum, and 2 when the SI was brighter than that of the cranial nerves or cerebellum. If any case was evaluated several times, the data from the latest evaluation were adapted. In addition, if cases with a score of 2 were evaluated several times, all scores were evaluated. Examples of CM-T1SI score evaluations are shown in Fig. 1.

To quantitatively evaluate the CM-T1SI ratio, the contrast ratio (CR) between the CM and cerebellar white matter was measured bilaterally by drawing a region of interest (ROI) on the 3D-SPGR T1WI. The ROI for the CM was defined as a circle enclosing 1 mm<sup>2</sup>. The ROI for the cerebellar white matter was defined as a circle enclosing 100 mm<sup>2</sup>. The CR value was defined as the CM signal divided by that of the cerebellar white matter on the same side. Representative ROIs on SPGR T1WI are shown in Fig. 2.

### Statistical analysis

We analyzed the differences in CM-T1SI scores and ratios between the i-SS, s-SS, and NC groups using Kruskal–Wallis tests followed by Mann–Whitney U

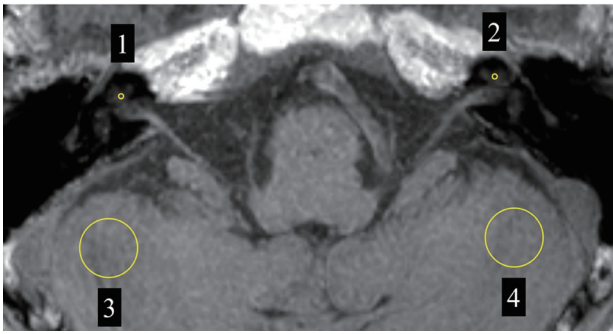


**Fig. 2.** An example of the regions of interest (ROIs) definition. The ROIs (1 and 2) are placed in the bilateral cochlear modiolus (CM). Each ROI in the CM is defined with an area of 1 mm<sup>2</sup>. ROIs (3 and 4) are placed bilaterally in the cerebellar hemispheres. Each ROI in the cerebellar hemispheres is defined with an area of 100 mm<sup>2</sup>.

tests. Next, the correlations between the CM-T1SI scores and ratios were statistically analyzed using Spearman's rank-order correlation coefficient tests.

For the differentiation of i-SS from NC, the cutoff values that provided the best combination of sensitivity and specificity for CM-T1SI scores and ratios were selected using receiver operating characteristic (ROC) analysis. The cutoff values were determined using the Youden index. We determined the accuracy, sensitivity, specificity, positive predictive value, and negative predictive value of each parameter using chi-square analysis. The area under the ROC curve (Az) was also evaluated for each parameter. The evaluations for the differentiation of s-SS from NC were performed as previously described if significant differences in CM-T1SI scores and ratios were observed between the s-SS and NC groups.  $P < 0.01$  was considered indicative of a statistical significance.

All statistical analyses were performed using EZR (Saitama Medical Center, Jichi Medical University, Saitama, Japan), a graphical user interface for R (The R Foundation for Statistical Computing, Vienna, Austria).<sup>13</sup>

## RESULTS

The CM-T1SI scores and ratios are shown in Tables 2 and 3. Scatterplots of the CM-T1SI scores and ratios are shown in Fig. 3. Scatterplots of the correlations between the CM-T1SI score and ratio are shown in Fig. 4.

Hearing loss was observed in two of the three patients in the i-SS group and in no cases in the s-SS group. Regarding CM-T1SI scores, a score of 0 was observed in 39 of 46 regions in the NC group, in 12 of 16 regions in the s-SS group, and in no region in the

i-SS group. A score of 1 was observed in 7 of 46 regions in the NC group, 4 of 16 regions in the s-SS group, and 3 of 6 regions in the i-SS group. A score of 2 was only seen in three of the six regions of the i-SS group. The right CM in Case 1 with i-SS showed a score of 2 in both examinations performed over 8 months. In addition, bilateral CM in Case 3 in the i-SS group showed a score of 2 on all four examinations over 7.5 years.

The CM-T1SI score and ratio differed significantly between the three groups ( $P < 0.001$ ). Significant differences were also observed between the i-SS and NC groups ( $P < 0.001$ ) and between the i-SS and s-SS groups ( $P < 0.001$ ). We observed no significant difference in these two parameters between the s-SS and NC groups. In addition, the CM-T1SI score showed a significant positive correlation with the CM-T1SI ratio ( $P < 0.001$ ,  $\rho = 0.668$ ).

The results of the diagnostic tests of CM-T1SI score and ratio for the differentiation of i-SS from NC are summarized in Table 4. For a CM-T1SI score cutoff value of 1, ROC analyses showed an accuracy of 92.4% for the discrimination of i-SS from NC. The Az value was 0.962. For a CM-T1SI ratio cutoff value of 0.628, the accuracy of discriminating i-SS from NC was 98.9%. The Az value was 0.996. ROC analyses were not performed for discriminating s-SS from NC because these two parameters did not differ significantly between the s-SS and NC groups. Representative images of 3D-SPGR T1WI and T2\*WI for each group are shown in Figs. 5–8.

## DISCUSSION

Our study evaluated the correlation between SS and high SI of the CM on unenhanced thin-sliced T1WI. Regarding CM-T1SI scores, a score of 2 (high SI of the CM), was only seen in the i-SS group. Furthermore, a score of 0 (low SI of the CM) was not observed in the i-SS group. In addition, the CM-T1SI score showed a significant positive correlation with the CM-T1SI ratio. The CM-T1SI ratio showed a 98.9% accuracy for discriminating the i-SS group from the control group at a cutoff value of 0.628. Therefore, our findings revealed a correlation between i-SS and high SI of the CM on T1WI. To our knowledge, this finding has not previously been reported. This may be related to the slice thickness of T1WI; if previous studies had been evaluated by conventional T1WI using such as 5-mm-thick sections for cases with i-SS, thicker slices could result in averaging of the signal void of bone with the high SI of the CM to yield an intermediate SI, thus, failing to show high SI in the CM. Therefore, our results using thin-sliced T1WI can be an additional characteristic finding of i-SS.

**Table 2. Summary of magnetic resonance (MR) findings for superficial siderosis**

Case	Age/ Sex	Causative disorders	HL	Type of SS	Supratentorial hemosiderin deposition	Infratentorial hemosiderin deposition	CM side	CM T1SI score	CM T1SI ratio
1	69/M	Metastatic tumor of the left frontal lobe	-	i	+	+	Right	2	0.976
							Left	1	0.628
2	77/F	Cavernous hemangioma of the 3rd ventricle	+	i	+	+	Right	1	0.792
							Left	1	0.772
3	44/F	Cystic lesion of the temporal lobe	+	i	+	+	Right	2	0.979
							Left	2	1.123
4	76/F	Traumatic SAH	-	s	+	-	Right	0	0.441
							Left	0	0.413
5	75/M	After resection of the convexity meningioma	-	s	+	-	Right	0	0.424
							Left	0	0.521
6	79/M	After resection of the convexity meningioma	-	s	+	-	Right	1	0.622
							Left	0	0.577
7	58/M	Traumatic SAH	-	s	+	-	Right	0	0.601
							Left	1	0.781
8	85/M	Traumatic SAH	-	s	+	-	Right	0	0.468
							Left	0	0.6
9	71/M	Traumatic SAH	-	s	+	-	Right	0	0.501
							Left	0	0.686
10	78/M	Anticoagulation-associated SAH	-	s	+	-	Right	0	0.36
							Left	0	0.53
11	77/M	Aneurysmal SAH	-	s	+	-	Right	1	0.614
							Left	1	0.629

CM, cochlear modiolus; F, female; HL, hearing loss; i, infratentorial; M, male; s, supratentorial; SS, superficial siderosis; T1SI, T1-weighted signal intensity

**Table 3. CM T1SI score and ratio in the i-SS, s-SS, and NC groups**

	i-SS group	s-SS group	NC group	<i>P</i> -value (Kruskal-Wallis Test)
	Score (number)	Score (number)	Score (number)	
CM T1SI score	0 (0), 1 (3), 2 (3)	0 (12), 1 (4), 2 (0)	0 (39), 1 (7), 2 (0)	<i>P</i> < 0.001
	Range (median)	Range (median)	Range (median)	
CM T1SI ratio	0.628-1.223 (0.884)	0.36-0.781 (0.556)	0.404-0.642 (0.499)	<i>P</i> < 0.001

CM, cochlear modiolus; i, infratentorial; NC, normal control; s, supratentorial; SS, superficial siderosis; T1SI, T1-weighted signal intensity.

The mechanisms by which i-SS causes high SI of the CM on T1WI remain unclear. The possible explanations for high SI on unenhanced T1WI include fat, slow flow, high protein content, and prior hemorrhage.<sup>12</sup> According to previous studies, high SI in the otic labyrinth can be caused by methemoglobin in subacute-stage

hematomas (intralabyrinthine hemorrhage) in patients with sudden hearing loss and vertigo.<sup>12, 14, 15</sup> However, the signal change can be seen not only in the CM but also in various regions of the otic labyrinth, including the cochlea, vestibule, and semicircular canals.<sup>12, 14, 15</sup> Weissman et al. reported that the high SI of the otic



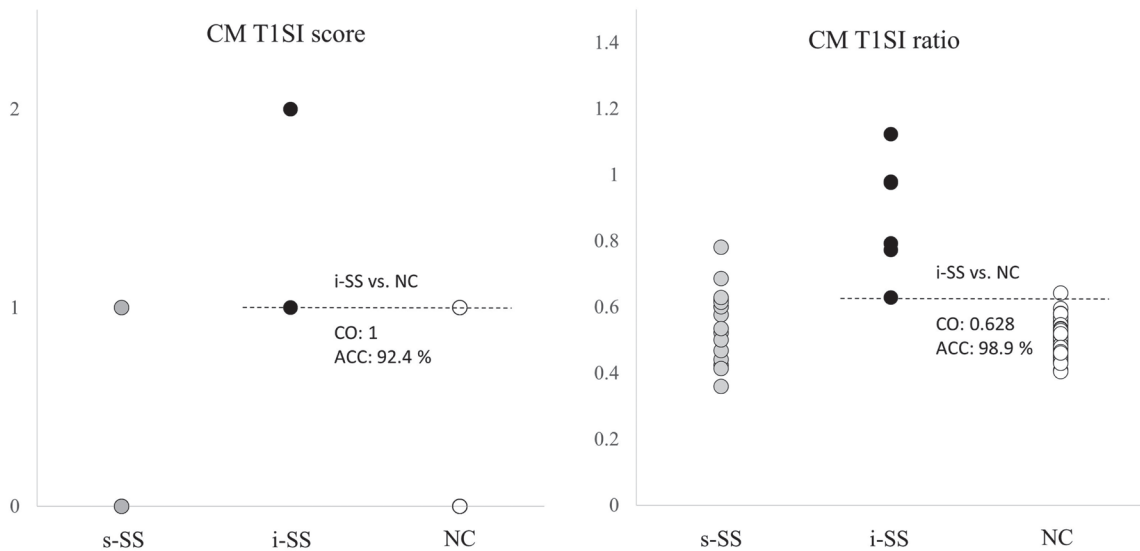


**Fig. 3.** Scatterplots of the CM T1SI score and ratio. ACC, accuracy; CM, cochlear modiolus; CO, cutoff value; i, infratentorial; NC, normal control; s, supratentorial; SS, superficial siderosis; T1SI, T1 signal intensity.

**Table 4. The diagnostic tests for CM T1SI score and ratio in differentiating the i-SS group from the NC group**

	AUC	Cutoff value	ACC	SEN	SPE	PPV	NPV	P-value
CM T1SI score	0.962	1	92.4%	100%	84.7%	86.7%	100%	$P < 0.001$
CM T1SI ratio	0.996	0.628	98.9%	100%	97.8%	97.8%	100%	$P < 0.001$

ACC, accuracy; AUC, area under the curve; CM, cochlear modiolus; i, infratentorial; NC, normal control; NPV, negative predictive value; PPV, positive predictive value; SEN, sensitivity; SPE, specificity; SS, superficial siderosis; T1SI, T1-weighted signal intensity.

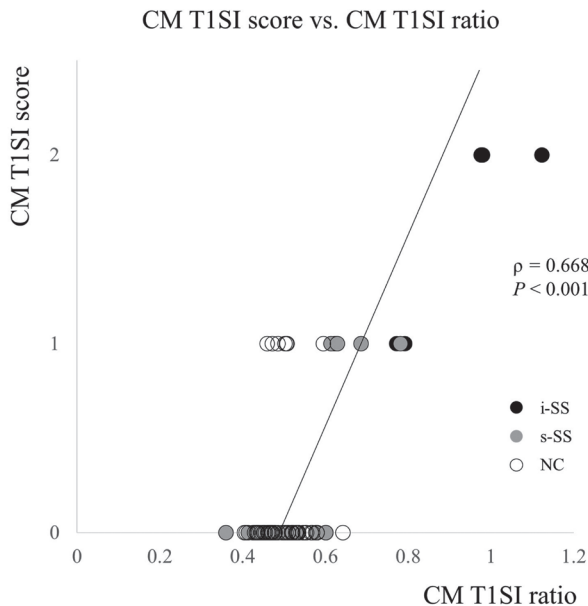


**Fig. 4.** Scatterplots of the correlations between CM T1SI score and ratio. The CM T1SI score is significantly positively correlated with the CM T1SI ratio ( $P < 0.001$ ,  $\rho = 0.668$ ). CM, cochlear modiolus; i, infratentorial; NC, normal control; s, supratentorial; SS, superficial siderosis; T1SI, T1 signal intensity.

labyrinth had decreased in follow-up scans of chronic-stage intralabyrinthine hemorrhages, and speculated that that finding had resulted from hematoma turnover in the labyrinth, gradually diluting or clearing the blood.<sup>12</sup> In this study, the high SI localized in the CM in cases with i-SS (Cases 1 and 3) persisted for 8 months and 7.5 years, respectively. Consequently, the mechanism of high SI of the CM in cases with i-SS may differ from that of temporary high SI of the otic labyrinth observed in intralabyrinthine hemorrhage.

The CM is highly porous and allows communication between the perilymph and the perivascular and perineural space in the CM, serving as the interscalar communication route as well as a communication route between the perilymph and cerebrospinal fluid (CSF).<sup>16, 17</sup> Pathologically, this communication is an important potential route for spreading infection, dissemination, and subarachnoid hemorrhage.<sup>18, 19</sup> In this study, high SI of the CM on TIWI was observed for i-SS but not s-SS. Therefore, in i-SS, components from dens hemosiderin deposition of the posterior fossa may chronically spread to the CM via the CSF. However, direct hemosiderin deposition to the CM is unlikely

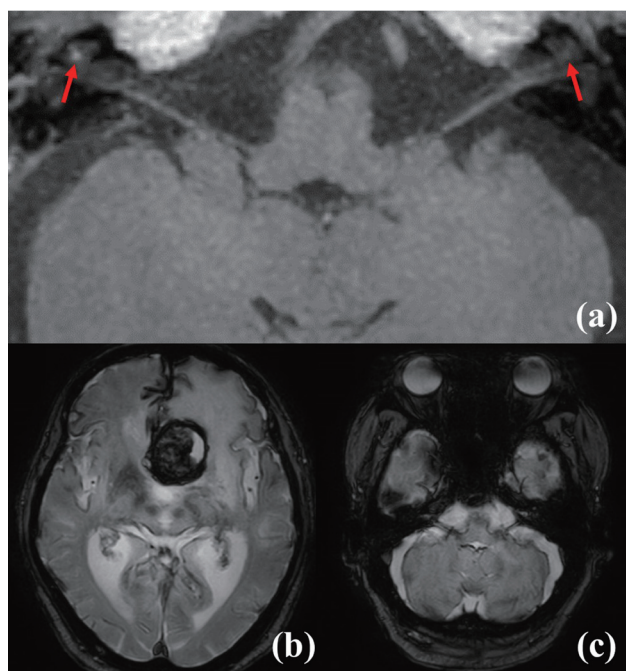


**Fig. 5.** Representative magnetic resonance (MR) images of infratentorial superficial siderosis (i-SS) with high and iso signal intensities (SIs) of the cochlear modiolus (CM) in Case 1 (a 69-year-old man). (a) Axial three-dimensional spoiled gradient-recalled (3D-SPGR) T1WI shows high SI in the right CM (score 2) and iso SI in the left CM (score 1) compared to the SI of the cranial nerves or cerebellum. (b) Axial T2\*WI shows dense low SI, which delineates the surfaces of the frontal lobes, temporal lobes, and midbrain. A cystic mass lesion with a dense, low-SI rim in the left frontal base is also observed. The mass lesion was histologically diagnosed as a metastatic thyroid carcinoma. (c) Axial T2\*WI shows dense low SI, which delineates the surfaces of the pons and cerebellum.

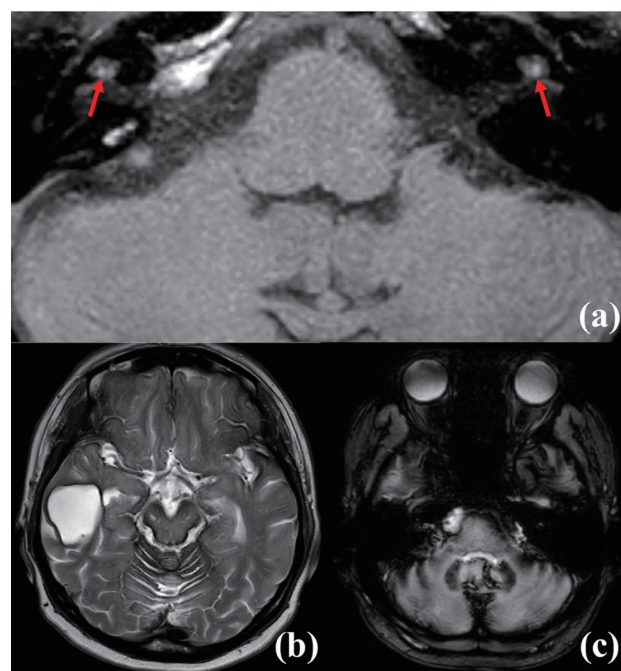


**Fig. 6.** Representative magnetic resonance (MR) images of infratentorial superficial siderosis (i-SS) with high signal intensity (SI) of the cochlear modiolus (CM) in Case 3 (a 44-year-old woman). (a) Axial three-dimensional spoiled gradient-recalled (3D-SPGR) T1WI shows high SI of the bilateral CM (score 2) compared to the SIs of the cranial nerves or cerebellum. (b) Axial T2\*WI shows dense low SI, which delineates the surfaces of the frontal lobes, temporal lobes, midbrain, and cerebellum. A cystic lesion with a dense low SI rim in the right temporal lobe is also observed. The lesion was not histologically diagnosed. (c) Axial T2\*WI shows dense low SI, which delineates the surfaces of the pons and cerebellum.

to reflect the high SI of the CM because hemosiderin usually shows low SI on T1WI. Therefore, unknown materials, including ferritin associated with hemosiderin, or tissue reactions, including glial reactions, to hemosiderin deposition could have been responsible for the persistent high SI of the CM on T1WI in cases with i-SS. However, no case in this study had histologic proof of these proposed findings.

Our study had several limitations. First, this retrospective study was conducted at a single hospital; thus, the study population was small. Second, only three cases of i-SS and eight cases of s-SS evaluated by 3D-SPGR T1WI were reviewed because most cases with SS were excluded owing to the evaluation of fast spin-echo T1WI using 5-mm-thick sections. Third, the ear symptoms, clinical history, and various otological tests performed by experienced otorhinolaryngologists were not evaluated in all cases due to the retrospective nature of the study. As the eighth cranial nerve is particularly

vulnerable in i-SS owing to its long glial segment, which results in greater hemosiderin deposition and a greater chance of axonal damage,<sup>1,20</sup> it may be difficult to evaluate whether high SI in the CM contributes to hearing loss. Due to these limitations, further validation with a larger number of cases is needed. Despite these limitations, we believe that our findings provide additional insights for the diagnostic workup of i-SS.

In conclusion, high SI of the CM on unenhanced thin-sliced T1WI can be an additional characteristic finding of i-SS.

*Acknowledgments:* We are grateful for the expert assistance from the members of the Department of Radiological Technology, Tottori Prefectural Central Hospital.

*The authors declare no conflict of interest.*

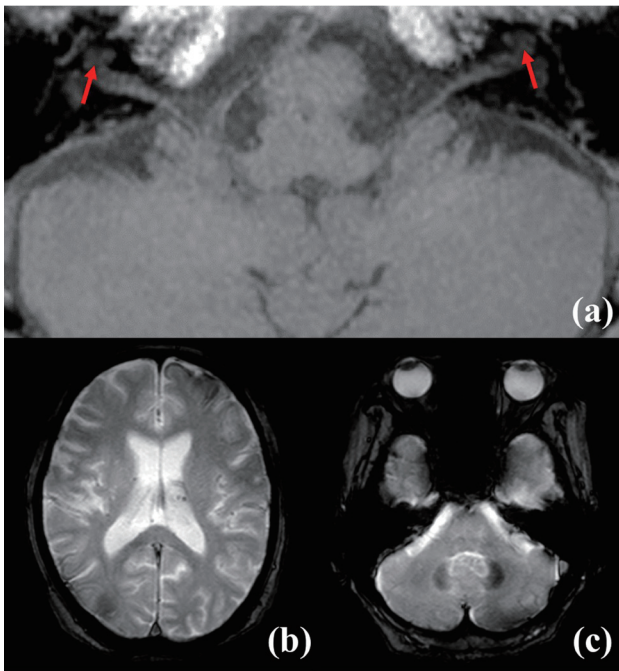


**Fig. 7.** Representative magnetic resonance (MR) images of supratentorial superficial siderosis (s-SS) with low signal intensity (SI) of the cochlear modiolus (CM) in Case 4 (76-year-old woman). (a) Axial three-dimensional spoiled gradient-recalled (3D-SPGR) T1WI shows low SI of the bilateral CM (score 0) compared to the SI of the cranial nerves and cerebellum. (b) Axial T2\*WI shows dense low SI, which delineates the surfaces of the left frontal and the right parietooccipital lobes. (c) Axial T2\*WI shows no low SI, which delineates the surfaces of the pons and cerebellum.

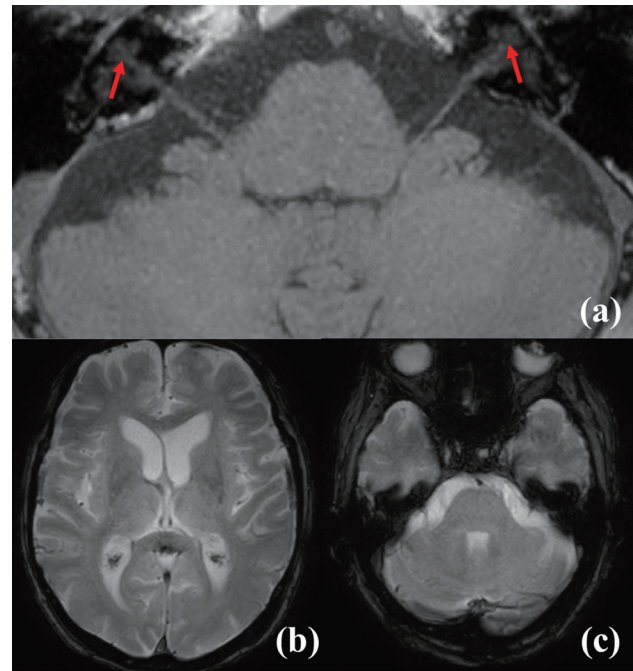


**Fig. 8.** Representative magnetic resonance (MR) images of a normal control case (an 83-year-old man) with the low signal intensity (SI) of the cochlear modiolus (CM). (a) Axial three-dimensional spoiled gradient-recalled (3D-SPGR) T1WI shows low SI of the bilateral CM (score 0) compared to the SI of the cranial nerves and cerebellum. (b and c) Axial T2\*WI shows no low SI, which delineates the surfaces of the cerebral hemisphere (b) and the surfaces of the pons and cerebellum (c).

## REFERENCES

- 1 Fearnley JM, Stevens JM, Rudge P. Superficial siderosis of the central nervous system. *Brain*. 1995;118:1051-66. DOI: [10.1093/brain/118.4.1051](https://doi.org/10.1093/brain/118.4.1051), PMID: 7655881
- 2 Kumar N. Superficial siderosis. *Arch Neurol*. 2007;64:491-6. DOI: [10.1001/archneur.64.4.491](https://doi.org/10.1001/archneur.64.4.491), PMID: 17420310
- 3 Posti JP, Juvela S, Parkkola R, Roine S. Three cases of superficial siderosis of the central nervous system and review of the literature. *Acta Neurochir (Wien)*. 2011;153:2067-73. DOI: [10.1007/s00701-011-1116-0](https://doi.org/10.1007/s00701-011-1116-0), PMID: 21822983
- 4 Kumar N. Neuroimaging in superficial siderosis: an in-depth look. *AJNR Am J Neuroradiol*. 2010;31:5-14. DOI: [10.3174/ajnr.A1628](https://doi.org/10.3174/ajnr.A1628), PMID: 19729538
- 5 Yamawaki T, Sakurai K. Diagnosis and treatment of superficial siderosis. *Brain Nerve*. 2013;65:843-55. PMID: 23832987 Japanese with English abstract.
- 6 Levy M, Turtzo C, Llinas RH. Superficial siderosis: a case report and review of the literature. *Nat Clin Pract Neurol*. 2007;3:54-8. DOI: [10.1038/ncpneu0356](https://doi.org/10.1038/ncpneu0356), PMID: 17205075
- 7 Wilson D, Chatterjee F, Farmer SF, Rudge P, McCarron MO, Cowley P, et al. Infratentorial superficial siderosis: Classification, diagnostic criteria, and rational investigation pathway. *Ann Neurol*. 2017;81:333-43. DOI: [10.1002/ana.24850](https://doi.org/10.1002/ana.24850), PMID: 28019651
- 8 Reuck JLD. Cortical superficial siderosis of the central nervous system - An overview. *Eur Neurol Rev*. 2014;9:68-70. DOI: [10.17925/ENR.2014.09.01.68](https://doi.org/10.17925/ENR.2014.09.01.68)
- 9 Offenbacher H, Fazekas F, Schmidt R, Kapeller P, Fazekas G. Superficial siderosis of the central nervous system: MRI findings and clinical significance. *Neuroradiology*. 1996;38(suppl 1):S51-6. DOI: [10.1007/BF02278119](https://doi.org/10.1007/BF02278119), PMID: 8811680
- 10 Charidimou A, Peeters A, Fox Z, Gregoire SM, Vandermeeren Y, Laloux P, et al. Spectrum of transient focal neurological episodes in cerebral amyloid angiopathy: multicentre magnetic resonance imaging cohort study and meta-analysis. *Stroke*. 2012;43:2324-30. DOI: [10.1161/STROKEAHA.112.657759](https://doi.org/10.1161/STROKEAHA.112.657759), PMID: 22798323
- 11 Sakurai K, Tokumaru AM, Nakatsuka T, Murayama S, Hasebe S, Imabayashi E, et al. Imaging spectrum of sporadic cerebral amyloid angiopathy: multifaceted features of a single pathological condition. *Insights Imaging*. 2014;5:375-85. DOI: [10.1007/s13244-014-0312-x](https://doi.org/10.1007/s13244-014-0312-x), PMID: 24519790
- 12 Weissman JL, Curtin HD, Hirsch BE, Hirsch WL Jr. High signal from the otic labyrinth on unenhanced magnetic resonance imaging. *AJNR Am J Neuroradiol*. 1992;13:1183-7. PMID: 1636533
- 13 Kanda Y. Investigation of the freely available easy-to-use software 'EZR' for medical statistics. *Bone Marrow Transplant*. 2013;48:452-8. DOI: [10.1038/bmt.2012.244](https://doi.org/10.1038/bmt.2012.244), PMID: 23208313



- 14 Lee JW, Park YA, Park SM, Kong TH, Park SY, Bong JP, et al. Clinical features and prognosis of sudden sensorineural hearing loss secondary to intralabyrinthine hemorrhage. *J Audiol Otol.* 2016;20:31-5. DOI: [10.7874/jao.2016.20.1.31](https://doi.org/10.7874/jao.2016.20.1.31), PMID: [27144231](https://pubmed.ncbi.nlm.nih.gov/27144231/)
- 15 Jrad M, Zlitni H, Boumediene M, Nasr AB, Bouzrara M. Intracochlear hemorrhage: A rare cause of sudden sensorineural hearing loss. *Case Rep Radiol.* 2021;2021:1-4. DOI: [10.1155/2021/1072047](https://doi.org/10.1155/2021/1072047), PMID: [34853709](https://pubmed.ncbi.nlm.nih.gov/34853709/)
- 16 Rask-Andersen H, Schrott-Fischer A, Pfaller K, Glueckert R. Perilymph/modiolar communication routes in the human cochlea. *Ear Hear.* 2006;27:457-65. DOI: [10.1097/01.aud.0000233864.32183.81](https://doi.org/10.1097/01.aud.0000233864.32183.81), PMID: [16957497](https://pubmed.ncbi.nlm.nih.gov/16957497/)
- 17 Kawai H, Naganawa S, Ishihara S, Sone M, Nakashima T. MR imaging of the cochlear modiulus after intratympanic administration of Gd-DTPA. *Magn Reson Med Sci.* 2010;9:23-9. DOI: [10.2463/mrms.9.23](https://doi.org/10.2463/mrms.9.23), PMID: [20339263](https://pubmed.ncbi.nlm.nih.gov/20339263/)
- 18 Aikawa T, Ohtani I. Temporal bone findings in central nervous system leukemia. *Am J Otolaryngol.* 1991;12:320-5. DOI: [10.1016/0196-0709\(91\)90027-D](https://doi.org/10.1016/0196-0709(91)90027-D), PMID: [1812774](https://pubmed.ncbi.nlm.nih.gov/1812774/)
- 19 Naganawa S, Satake H, Iwano S, Sone M, Nakashima T. Communication between cochlear perilymph and cerebrospinal fluid through the cochlear modiulus visualized after intratympanic administration of Gd-DTPA. *Radiat Med.* 2008;26:597-602. DOI: [10.1007/s11604-008-0286-z](https://doi.org/10.1007/s11604-008-0286-z), PMID: [19132490](https://pubmed.ncbi.nlm.nih.gov/19132490/)
- 20 Ushio M, Iwasaki S, Sugasawa K, Murofushi T. Superficial siderosis causing retrolabyrinthine involvement in both cochlear and vestibular branches of the eighth cranial nerve. *Acta Otolaryngol.* 2006;126:997-1000. DOI: [10.1080/00016480500540535](https://doi.org/10.1080/00016480500540535), PMID: [16864501](https://pubmed.ncbi.nlm.nih.gov/16864501/)